KSÜ Mühendislik Bilimleri Dergisi, 28(2), 2025
Araştırma Makalesi

KSU J Eng Sci, 28(2), 2025
Research Article

Kahramanmaras Sutcu Imam University
Journal of Engineering Sciences

Geliş Tarihi : 05.01.2025
Kabul Tarihi : 18.03.2025

Received Date : 05.01.2025
Accepted Date : 18.03.2025

DEEP LEARNING METHODOLOGIES FOR NUCLEI SEGMENTATION AND MITOSIS DETECTION IN HISTOPATHOLOGICAL IMAGES ANALYSIS

HİSTOPATOLOJİK GÖRÜNTÜ ANALİZİNDE ÇEKİRDEK SEGMENTASYONU VE MİTOZ TESPİTİ İÇİN DERİN ÖĞRENME YÖNTEMLERİ

Refik SAMET[1] (ORCID: 0000-0001-8720-6834)
Nooshin NEMATİ[1*] (ORCID: 0000-0002-5306-0344)
Emrah HANCER[2,3] (ORCID: 0000-0002-3213-5191)
Serpil SAK[4] (ORCID: 0000-0003-3666-3095)
Bilge Ayca KİRMİZİ[4] (ORCID: 0000-0003-3192-1921)
Zeynep YİLDİRİM[1] (ORCID: 0000-0001-5846-9256)

[1]Ankara University, Department of Computer Engineering, Ankara, Turkiye
[2]Victoria University of Wellington, School of Engineering and Computer Science, Wellington, New Zealand
[3]Mehmet Akif Ersoy University, Department of Software Engineering, Burdur, Turkiye
[4]Ankara University, Department of Pathology, Ankara, Turkiye.

*Sorumlu Yazar / Corresponding Author: Nooshin NEMATİ, nntolakan@ankara.edu.tr

ABSTRACT

Histopathological image analysis is a pivotal area of medical research that leverages deep learning to derive quantitative insights from Hematoxylin and Eosin (H\&E) stained images. This study aims to enhance the analysis of H\&E breast cancer histopathology images by developing deep learning methodologies focused on nuclei and mitosis. Nuclei provide essential information for disease diagnosis, while mitosis is crucial for cancer grading and prognosis prediction. We propose two methodologies: the first segments nuclei using a U-shaped semantic segmentation architecture called CompSegNet; the second detects and classifies mitotic cells through a hybrid approach combining object detection and fuzzy classification algorithms. To evaluate the effectiveness of these methodologies, we introduce two new publicly available datasets: NuSeC (Nuclei Segmentation and Classification) and MiDeSeC (Mitosis Detection, Segmentation, and Classification). These datasets not only validate our methodologies but also provide valuable resources for developing deep learning models in histopathological image analysis.

Keywords: Breast cancer, digital pathology, mitosis detection, nuclei segmentation, histopathology.

ÖZET

Histopatolojik görüntü analizi, Hematoksilin ve Eozin (H&E) boyalı görüntülerden nicel bilgiler elde etmek için derin öğrenmeyi kullanan tıbbi araştırmaların önemli bir alanıdır. Bu çalışma, H&E ile boyanmış meme kanseri histopatoloji görüntülerinin analizini, çekirdekler ve mitoz üzerine odaklanmış derin öğrenme metodolojileri geliştirerek geliştirmeyi amaçlamaktadır. Çekirdekler, hastalık teşhisi için hayati bilgiler sağlarken, mitoz, kanser derecelendirmesi ve prognoz tahmini için kritik öneme sahiptir. İki metodoloji öneriyoruz: Birincisi, çekirdekleri CompSegNet adlı U-şekilli bir anlamsal segmentasyon mimarisi kullanarak segment emektedir; ikincisi ise mitotik hücreleri tespit edip sınıflandırmak için nesne tespiti ve bulanık sınıflandırma algoritmalarını birleştiren hibrit bir yaklaşım uygulamaktadır. Bu metodolojilerin etkinliğini değerlendirmek için, kamuya açık iki yeni veri seti sunuyoruz: NuSeC (Çekirdek Segmentasyonu ve Sınıflandırması) ve MiDeSeC (Mitoz Tespiti, Segmentasyonu ve Sınıflandırması). Bu veri setleri, yalnızca metodolojilerimizi doğrulamakla kalmayıp, aynı zamanda histopatolojik görüntü analizi için derin öğrenme modellerinin geliştirilmesine yönelik değerli kaynaklar sunmaktadır.

Anahtar Kelimeler: Meme kanseri, dijital patoloji, mitoz tespiti, çekirdek segmentasyonu, histopatoloji.

ToCite: SAMET, S., NEMATİ, N., HANCER, E., SAK, S., KİRMİZİ. B.A., & YİLDİRİM, Z., (2025). DEEP LEARNING METHODOLOGIES FOR NUCLEI SEGMENTATION AND MITOSIS DETECTION IN HISTOPATHOLOGICAL IMAGES ANALYSIS. *Kahramanmaraş Sütçü İmam Üniversitesi Mühendislik Bilimleri Dergisi*, 28(2), 785-801.

INTRODUCTION

Histopathological image analysis represents a pivotal frontier in medical research, leveraging computer algorithms to extract quantitative insights from histopathological images. This transformative process extracts crucial information for disease diagnosis, tumor grading, and treatment response assessment. Specifically, Hematoxylin and Eosin (H\&E) stained images, a prevalent category of histopathological imagery, utilize dual dyes, hematoxylin and eosin, to highlight distinct cellular components. Hematoxylin imparts a blue hue to cell nuclei, while eosin imparts a pink shade to cell cytoplasm and interstitial tissue, including collagen fibers (Chen et al., 2018). The intricacies of this staining process bring forth diverse tissue structures, notably nuclei and mitosis, which are essential for diagnosing and categorizing numerous diseases.

Nuclei segmentation is a cornerstone in histopathological image analysis, representing the initial stride toward extracting quantitative information about cellular composition, morphology, and pathological alterations within tissues. This process facilitates the identification and segmentation of cancerous nuclei based on size, shape, and texture, gauges cancer stage by quantifying the size and quantity of cancerous nuclei, and contributes to cancer grading by assessing the aggressiveness of these cells, ultimately providing invaluable information for predicting patient prognosis (Naylor et al., 2017). The meticulous analysis of nuclei in H\&E histopathology images is imperative for precise diagnoses, offering profound insights into cell and tissue health and function.

Mitosis is the process by which a single parent cell divides to produce two identical daughter cells. This carefully controlled event occurs in all eukaryotic cells. When evaluating mitosis in breast and other human tumors, pathologists typically examine H\&E-stained sections within a standardized area. Detecting mitosis in histopathological image analysis serves various purposes, especially in the diagnosis and grading of cancer. The mitotic count, which reflects the number of mitotic cells in a given tissue area, is associated with tumor aggressiveness and patient prognosis (Swarts et al., 2014). Accurate evaluation requires robust tissue fixation and processing to focus on definitive mitoses while distinguishing them from apoptotic cells and artifacts.

Recent advancements in deep learning have marked substantial progress in nuclei segmentation and mitosis detection within histopathological image analysis (Sohail et al., 2021). These methods are capable of comprehending intricate features of nuclei and mitotic cells, achieving remarkable accuracy and precision. Despite this progress, several challenges persist, including variability in nuclear shapes, sizes, staining intensities, overlapping nuclei, and artifacts (Khan et al., 2021). Moreover, deep learning models are prone to overfitting, particularly with small or non-representative datasets, which may lead to excellent performance on training data but poor generalization to new data. The clinical applicability of these methods remains limited due to inconsistencies in annotation quality and the need for more robust and generalizable models (Nemati et al., 2023).

To address these issues, we propose deep-learning methodologies for histopathological image analysis. The proposed methodology for nuclei segmentation initially employs multiple data preprocessing strategies to standardize and enhance image quality, ensuring consistency across datasets. Following preprocessing, it utilizes a recently introduced U-shaped architecture called CompSegNet to effectively capture both local and global features for accurate nuclei segmentation (Traoré et al., 2024). The second methodology focuses on mitosis detection and begins with Macenko color normalization to reduce staining variations and improve image uniformity, which is crucial for reliable detection across diverse samples. Then it uses the YOLOv8 architecture to accurately identify mitotic cells. Finally, fuzzy-based classification algorithms are used to classify the detected mitoses, leveraging their ability to manage uncertainties and overlapping class boundaries, thereby enhancing the robustness and accuracy of the classification process. Moreover, we introduce two publicly available datasets, NuSeC and MiDeSeC, designed for the development of robust models in nuclei segmentation and mitosis detection tasks.

The main contributions of the study can be summarized as follows:

- The introduction of nuclei segmentation methodology. It involves a preprocessing stage that normalizes image color variations and resizes images into non-overlapping patches, followed by the CompSegNet architecture, which includes an encoder for feature extraction, a Transformer bottleneck for integrating

information, a decoder for reconstructing segmentation maps, and a segmentation head for creating final nuclei masks.

- The introduction of mitosis detection methodology. It involves preprocessing with Macenko color normalization, detecting mitotic cells using YOLOv8, and classifying them with fuzzy-based algorithms to handle uncertainties and improve accuracy.
- The design of the NuSeC dataset comprises 100 images capturing over 6000 nuclei structures within breast cancer at a 40× magnification.
- The design of the MiDeSeC dataset, featuring 50 images with more than 500 mitosis structures within breast cancer at a 40× magnification.

The paper is structured as follows. Section 2 reviews pertinent literature on nuclei datasets and their applications in nuclei segmentation and mitosis detection. Section 3 details the materials and methods used in the study, while Section 4 presents the results and discussion. Finally, Section 5 concludes the paper and suggests future research directions.

RELATED WORKS

Review on Nuclei Segmentation and Mitosis Detection

Deep Learning Methods for Nuclei Segmentation Table 1 provides a comprehensive summary of various deep learning methods used for mitosis detection, listing the corresponding datasets and techniques implemented. The field has seen a diverse range of approaches, reflecting the continuous evolution and exploration of mitosis detection techniques. Several studies, such as those by (Hancer et al. 2023; Chen et al., 2020; Hassan et al., 2021), have employed the MoNuSeg dataset, utilizing methods like REMFA-Net, U-Net, and Efficient Stain-Aware. This variety underscores the importance of tailoring methodologies to specific dataset characteristics and the challenges posed by nuclei segmentation. The detailed descriptions of the corresponding methods are provided as follows.

Graham et al. (2019) presented a CNN model for automatic nuclear segmentation and classification in H\&E-stained histology images. The model utilizes the distances of nuclear pixels to their centers to separate clustered nuclei, ensuring accurate segmentation. It also includes a dedicated classification branch for nucleus type prediction. The method demonstrates superior performance across multiple datasets and introduces a new colorectal adenocarcinoma dataset with 24,319 annotated nuclei. Le Dinh et al. (2022) explored automated cell nuclei segmentation using deep learning. Nested U-Net with EfficientNet as the encoder implemented on CryonuSeg dataset. The model has achieved a Dice score of 0.929, AJI of 0.604, and PQ of 0.503. Chen et al. (2020) proposed REMFA-Net, an automatic nuclei segmentation method for histopathology images using rotation-equivariant and multi-level feature aggregation. It incorporates group equivariant convolutions for better segmentation and a U-Net3+ based strategy to bridge the semantic gap. Key innovations include a new decoder module, improved skip connections, and a semantic enhancement block. REMFA-Net has been evaluated on the MoNuSeg dataset.

Hancer et al. (2023) presented an imbalance-aware nuclei segmentation method for H\&E-stained histopathology images. It includes a preprocessing stage with resizing, augmentation, and normalization, along with a lightweight U-Net using a generalized Dice loss layer. Evaluated on the MoNuSeg2018 dataset. The method outperforms recent approaches in AJI and IoU metrics. Hassan Dinh et al. (2021) proposed a stain-aware nuclei segmentation method for multi-center WSIs using deep learning. Unlike single-stain normalization, it selects multiple stain templates via clustering and trains separate models for each. Segmentation masks are combined using the Choquet integral. The method outperforms approaches evaluated on a multi-center, multi-organ dataset, with an AJI of 0.7323 and an F1-score of 0.8932, while maintaining fewer parameters. Hoorali et al. (2022) proposed an improved UNet++ for microscopic tissue image segmentation. It has been enhanced with multi-scale feature fusion with new skip connections and integrates squeeze-and-excitation inception blocks. Various backbones strengthen feature extraction, while batch normalization, dropout, and LReLU improve convergence and generalization. A weighted hybrid loss addresses class imbalance, and marker-based watershed has been converted from semantic to instance segmentation. Khan et al. (2023) introduced TransUNet-Lite, a lightweight and efficient model for nuclei segmentation, addressing challenges such as variable image sizes and data imbalance. The model uses a convolution-based feature extractor, an external attention module, a fast token selector, and skip connections to maintain contextual information. It

processes patches instead of resized images to preserve aspect ratios. Evaluated on the 2018 Science Bowl dataset, TransUNet-Lite achieved a DSC of 0.9308 and IoU of 0.8795, outperforming state-of-the-art networks.

Table 1. A summary of deep-based methods for nuclei segmentation

Reference	Datasets	Methods
Hancer et al. (2023)	MoNuSeg	Lightweight U-Net
Chen et al., (2020)	MoNuSeg	REMFA-Net
Hlavcheva et al., (2019)	BreCaHAD	ConvNet
Aatresh et al., (2021)	TNBC	Kidney-SegNet
Liu et al. (2021)	TNBC	MDC-net
Hoorali et al., (2022)	MoNuSAC	Improved UNet++
Graham et al., (2019)	MoNuSAC	HoVer-Net
Ilyas et al., (2022)	PanNuke	TSFD-Net
Obeid et al., (2022)	PanNuke, CoNSep	NucDETR
Le Dinh et al., (2022)	CryonuSeg	Nested U-Net, EfficientNet
Hassan Dinh et al., (2021)	CryonuSeg, MoNuSeg	Efficient Stain-Aware
Khan et al. (2023)	Science Bowl	TransUNet-Lite

Deep Learning Methods for Mitosis Detection Table 2 summarizes different deep-based approaches employed for mitosis detection with their reference, datasets used, and methods employed. It is an attempt to learn and understand the current state of development in the field of mitosis detection, which is thematically heterogeneous. According to studies conducted by Khan et al. (2022**),** Yancey R (2023**),** and Maroof et al. (2020), the ICPR14 dataset was employed, wherein methods like SM-Detector, Faster R-CNN, Random Forest, and SVM were applied. These studies show that there should be careful selection of approaches that identify and address the unique identities of a dataset and can-do mitotic detection. (Yancey R, 2023) spread their investigation into both using YOLO and Faster R-CNN on the ICPR14 and ICPR12 datasets. This is an important move, suggesting that it realizes the need for robustness across the importance of using several architectures with different learning features, and various datasets, resulting in performance improvement. The detailed descriptions of the corresponding methods are provided as follows.

Dodballapur et al. (2019) presented a two-stage method for mitotic detection using cell masks. In the first stage, Mask R-CNN generates cell masks with high recall and low precision. The second stage refines detection by classifying cells as mitotic or non-mitotic using hand-crafted and deep features. Evaluated on ICPR 2012 and 2014 datasets, the method outperforms fully supervised segmentation and feature-based approaches, demonstrating effective mask transferability between datasets. Hamidinekoo et al. (2017) enhanced mitosis detection in breast histology images using RGB Histogram Specification for stain normalization. A modified deep CNN was trained on raw and normalized images across multiple datasets, improving staining and scanner variations robustness. Results showed a stable detection performance, enabling a generalizable mitosis detection model. Jahanifar et al. (2022) proposed a two-stage mitosis detection framework combining fast candidate segmentation (EUNet) and candidate refinement (EfficientNet-B7). EUNet accurately detects candidates at lower resolution, speeding up detection, while EfficientNet-B7 refines them. Domain generalization methods ensure robustness against domain shifts. The model achieves state-of-the-art performance on three large mitosis datasets, winning the MIDOG21 and MIDOG22 challenges. It also processes 1,124 TCGA breast cancer slides, generating over 620K potential mitotic figures. Khan et al. (2022) introduced SMDetector, a deep learning model for detecting small objects like mitotic and non-mitotic

nuclei in breast cancer images. It uses dilated layers in the backbone to prevent small objects from disappearing, improving detection. The model achieves an overall average precision (AP) of 0.5031 and average recall (AR) of 0.559, outperforming existing models on the ICPR 2014 (Mitos-Atypia-14) dataset. For mitotic nuclei, it achieves an AP of 0.6849, AR of 0.5986, and an F-measure of 0.6388. Maroof et al. (2020) addressed the challenge of nuclei segmentation in histopathology using transfer learning. The proposed approach leverages a pre-trained model as the backbone of a classical encoder-decoder architecture. A comparative study on the Triple Negative Breast Cancer dataset reveals that U-Net with EfficientNetB3 as the backbone performs best, improving the Dice score and Intersection over Union (IoU) values.

Table 2. A summary of deep-based methods for mitosis detection

Reference	Data sets	Methods
Khan et al., (2022)	ICPR14	SMDetector
Maroof et al., (2020)	ICPR14	Random Forest, SVM
Yancey R, (2023)	ICPR14, ICPR12	YOLO, Faster R-CNN
Li et al., (2018)	ICPR14, ICPR12	DeepMitosis
Dodballapur et al., (2019)	ICPR14, ICPR12	Mask R-CNN
Hamidinekoo et al., (2017)	ICPR14, AMIDA13	Faster R-CNN, YOLOv5
Sohail et al., (2021)	TUPAC16	MitosRes-CNN
Bertram et al., (2020)	TUPAC16	RetinaNet
Jahanifar et al., (2022)	MIDOG22	EUNet
Aubreville et al., (2023)	MIDOG21	RetinaNet

The different methods and datasets used still highlight the motivation to overcome the challenges of mitosis detection, such as inconsistencies in staining, dataset characteristics, and the need for accurate and robust detection across various datasets. This variety also indicates ongoing research into new architectures that integrate deep learning with traditional components, as well as modern algorithms like the Krill Herd Algorithm combined with fuzzy logic for decision-making processes. The advancements in both conventional and modern techniques demonstrate the necessity of diverse approaches to effectively address the challenges associated with mitosis detection in histopathological images.

Review on Histopathology Datasets

Review on Nuclei Datasets Table 3 offers a comprehensive overview of several key nuclei datasets utilized in histopathology image analysis. These datasets vary in terms of image sizes, magnifications, and sources. Some datasets, such as TNBC and CRYONUSEG, have been manually annotated, while others, like PanNuke and CoNSeP, use semi-automatic annotation. This highlights the differences in annotation quality among these datasets; for instance, the MoNuSeg dataset is recognized to have some annotation errors (Verdicchio et al., 2023). The TNBC and CRYONUSEG datasets have manual annotations; however, due to their relatively small size, they are not highly generalizable on their own. In contrast, PanNuke and CoNSeP, being much larger with semi-automated annotations, offer greater generalizability but may not achieve the same level of accuracy as manually annotated datasets. Additionally, the limited size of datasets like NuCLS (Amgad et al., 2022) constrains generalizability when training and evaluating deep learning models. Furthermore, breast cancer subtypes, such as the invasive ductal carcinoma, bias in the BCWD dataset (Wolberg & Mangasarian, 1992), present challenges in constructing generalizable models. Moreover, datasets like NuCLS suffer from significant annotation inconsistencies, which adversely affect the quality of training and evaluation in deep learning models. In conclusion, there is a pressing need for new breast cancer histopathology datasets that are larger, more diverse, and contain higher-quality annotations. Such datasets would support the development of more accurate and generalizable deep learning models for breast cancer diagnosis and prognosis.

Table 3. Nuclei datasets in literature

Datasets	Image size	Source	Nuclei Count	Organs Count
CoNSeP (Graham et al., 2019)	1000×1000	UHCW	24,319	1
MoNuSeg (Kumar et al., 2017)	1000×1000	TCGA	21,623	7
PanNuke (Gamper et al., 2020)	WSI	TCGA	205,343	19
MoNuSAC (Verma et al., 2020)	81×113,1422×2162	UHCW	46,909	4
CryoNuSeg (Mahbod et al., 2021)	512×512	TCGA	7,596	10
CPM-17 (Vu et al., 2019)	500×500 - 600×600	TCGA	7,570	4
CRCHisto (Sirin et al., 2016)	500×500	UHCW	29,756	1
NuCLS (Amgad et al., 2022)	WSI	TCGA	222,396	1
Lizard (Graham et al., 2021)	1,016×917	TCGA	495,179	1
TNBC (Naylor., 2018)	512×512	WSI	4,056	1

Review on Mitosis Datasets Table 4 provides a comprehensive review of datasets relevant to mitosis detection, detailing their magnification levels, scanner types, and image sizes. The ICPR12, AMIDA13, and ICPR14 datasets are relatively small, with a primary focus on breast cancer studies. In contrast, while the TUPAC16 dataset is larger, it lacks diversity in tissue types. The MIDOG21 and MIDOG22 datasets stand out as the largest and most diverse, featuring images from various scanners, tissue types, and species. However, the WSIs in MIDOG21 exhibit variability in tissue quality, including out-of-focus areas and regions with necrosis, introducing a diverse set of challenging negative examples that have not undergone formal evaluation. The MIDOG++ dataset represents the latest advancement, building upon MIDOG21 and MIDOG22. It includes a meticulously curated collection of Region of Interest (ROI) images extracted from 503 histological specimens, covering seven distinct tumor types with diverse morphological characteristics. The dataset contains an extensive set of 11,937 annotations specifically marking mitotic figures. While it aims for accuracy, the possibility of labeling errors or domain shifts in mitotic figures remains a consideration.

Table 4. Mitosis datasets in the literature

Datasets	Scanner	Image size	Cases
ICPR12 (Ludovic et al., 2013)	Scanner A&H, 10-band microscope	A:2084×2084, H:2250×2252, M:1360×1360	5
AMIDA13(Veta et al., 2014)	Scope XT scanner	2000×2000	23
ICPR14 (Roux et al., 2014)	scanner A&H	A:1539×1376, H:1663×1485	21
TUPAC16 (Veta et al., 2019)	Leica SCN400	2000×2000	73
MIDOG21(Wilm et al., 2021)	4 different Scanners	WSI	50
MIDOG22 (Aubreville et al., 2023)	5 different Scanners	WSI	403
MIDOG++ (Aubreville et al., 2023)	5 different Scanners	WSI	494

MATERIALS AND METHODS

Designed Histopathological Datasets

The datasets introduced for histopathological image analysis are presented as follows:

NuSeC Dataset This dataset was curated using H&E-stained breast tissue slides from 25 anonymous cases obtained from the Ankara University Faculty of Medicine, Department of Pathology archive. These patients underwent surgery (excisional biopsy, lumpectomy, or mastectomy) with a diagnosis of invasive breast carcinoma. The selected glass slides were scanned using a 3D HISTECH Panoramic Scanner P250 flash 3 to produce whole slide images (WSIs). A pathologist first marked regions with the highest nuclei activity. The most representative invasive tumor areas were selected, ensuring good fixation, high cellularity, and the absence of artifacts or necrosis.

The NuSeC dataset generation process is described as follows. In the first stage, image patches of 1024×1024 pixels were extracted from TIFF images in RGB 8-bit format. In the second stage, the nuclei of tumor cells in these patches were manually annotated one by one using QuPath (Bankhead et al., 2017), a tool designed for visualization, analysis, and annotation of WSIs in pathology. A pathologist from our research team reviewed the annotated tumor nuclei in the extracted patches. In the final stage, the resulting image files were appropriately named. This dataset was meticulously designed to represent a wide range of age groups, ensuring diversity and a comprehensive collection of breast tissue morphology. The NuSeC dataset consists of 100 images, with 75 allocated for training and 25 reserved for testing.

MiDeSeC Dataset This dataset was curated using H&E-stained breast tissue slides from 25 anonymous cases from the Ankara University Faculty of Medicine, Department of Pathology archive. The patients underwent surgery (excisional biopsy, lumpectomy, or mastectomy) with a diagnosis of invasive breast carcinoma. The selected glass slides were scanned using a 3D HISTECH Panoramic Scanner P250 flash 3 to obtain whole slide images (WSIs). A pathologist annotated the tumor areas on each slide, excluding stromal components and benign breast tissue from this study. Only the most representative invasive tumor areas with good fixation, high cellularity, and no artifacts or necrosis were selected. Typical and atypical mitotic figures within these tumor areas were identified and marked.

In the next stage, 1024×1024-pixel regions were cropped from these selected tumor fields and extracted in RGB 8-bit format from the TIFF images. The QuPath program was used to annotate these extracted patches, and the pathologist manually marked typical and atypical mitotic figures. Finally, the annotated images and their corresponding coordinate files (in Excel format) were prepared for use in deep learning algorithms. Two thirds of the images were reserved for training, with the remaining third for testing. Test and training sets were randomly selected.

Proposed Methodologies

The deep learning methodologies proposed for histopathological image analysis are presented as follows:

Nuclei Segmentation Methodology The structure of the suggested nuclei segmentation methodology is presented in Figure 1. The fundamental stages of the nuclei segmentation methodology are described as follows:

a) Preprocessing Stage: Preprocessing is applied to enhance image quality and prepare the data for segmentation. Images were resized to 1024×1024 pixels and divided into 256×256 non-overlapping patches for input into the architecture. Notice that color normalization was not applied to the NuSeC dataset, as it consists solely of single-organ tissue, which does not exhibit the color variations found in the other datasets.

b) Segmentation Stage: Due to its notable success in nuclei segmentation tasks, we selected CompSegNet (Traoré et al., 2024), a recently introduced U-shaped architecture. The CompSegNet architecture comprises four key components: the encoder, bottleneck, decoder, and segmentation head. The encoder transforms the input image into compact, low-dimensional feature representations. Acting as a bridge between the encoder and decoder, the bottleneck facilitates the transfer of information. The decoder then reconstructs the encoded representations into pixel-wise segmentations, restoring the original spatial resolution of the image. Finally, the segmentation head generates the final segmentation masks.

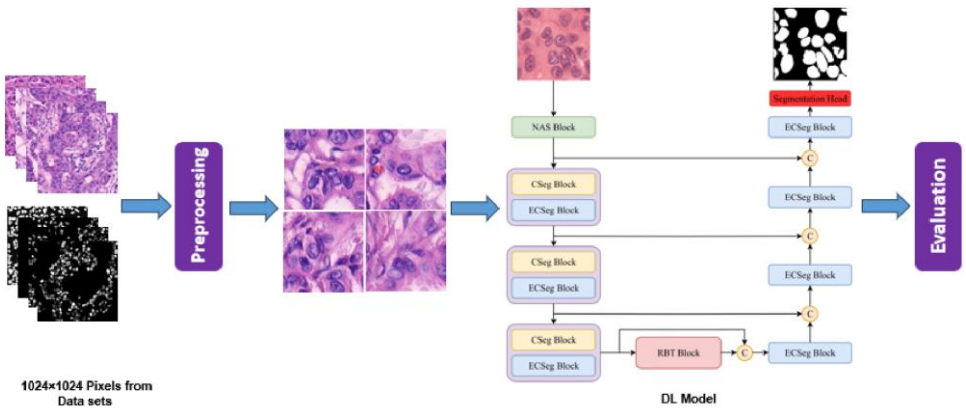

Figure 1. The overall structure of the nuclei segmentation methodology

The encoder begins with a stem block that processes an input image $I \in R^{H\times W\times 3}$, producing a feature map $f_1 \in R^{H\times W\times 3}$. This is followed by three encoder blocks that progressively reduce the spatial size of the feature map while increasing its channel dimensions. The final encoder block is followed by a Residual Bottleneck Transformer (RBT) block, which integrates the translation invariance and local sensitivity of CNNs with the global context encoding capability of Transformers. The decoder path upscales the encoded representations and concatenates them with corresponding feature maps from the encoder. The segmentation head then outputs the final mask, $f_{10} \in R^{H\times W\times N}$, where N represents the number of target classes.

CompSegNet (Traoré et al., 2024) has demonstrated superior performance in handling complex tissue structures, largely due to its ability to capture both local and global contextual information effectively. The architecture's use of CNNs for spatial feature extraction, combined with Transformers for capturing long-range dependencies, ensures accurate segmentation even in cases of overlapping nuclei and varying nuclear shapes and sizes. Moreover, the integration of a bottleneck layer enhances the network's ability to compress and process high-dimensional data efficiently, making it highly suitable for medical image segmentation tasks, where precision is critical (https://github.com/mltraore/CompSegNet).

Mitosis Detection Methodology The overall methodology for mitosis detection and classification from H&E-stained histopathology images is presented in Figure 2. The fundamental stages of the mitosis detection methodology are described as follows:

a) Preprocessing Stage: Macenko (Macenko et al., 2009) method is applied to find the stain vectors W in each image based on the color inside the tumor area. Since the Optical Density (OD) value is 0 when the corresponding light is not absorbed, the task is to find the minimum value and then use the corresponding pixels projected onto the geodesic direction as the two terminal stain vectors of the stain vectors. Macenko method is often used in the H&E-stained dyeing of histological images because it can erase the color difference very well, the texture features of the image become relevant, and the network robustness is improved.

b) Object Detection Stage: In the object detection stage, YOLOv8, a single-stage object detector, is employed. YOLOv8 architecture consists of three modules: backbone, neck, and head. Backbone, having pre-training weight, plays an important role in reducing the spatial resolution of the image and an increase feature resolution thereof through residual and dense blocks, which deal with vanishing gradient-type problems and enhance information flow. The backbone is mainly forms Composed of the convolution of too many C2f blocks, ending with SPPF. SPPF plays a critical role in saving parameters and computational resources that make the architecture suitable for real-time object detection tasks. The neck section deals with pyramidal feature extraction, allowing for a generalization of the model to objects of various sizes and scales. The neck feature incorporates 1 concatenation without any restriction on absolute channel numbers, thereby reducing effective model parameters and tensor size, thereby introducing efficiency. The head consists of two CNN layers producing class probabilities and the regression producing abjectness scores and bounding box coordinates. The CNN layers are configured with a 3×3 kernel size, a stride of 1, and padding of 1, ensuring precise localization of objects.

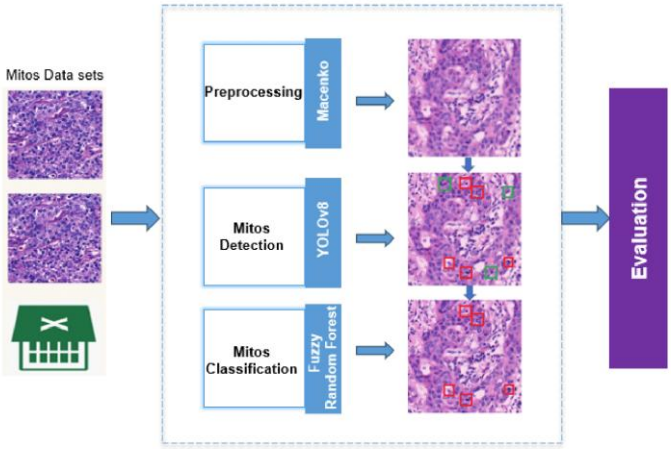

Figure 2. The overall structure of the mitosis detection methodology

YOLOv8 utilizes anchor box-free detection, which predicts the center of the object directly, leading to improvements in both accuracy and speed. With its 225 layers, 11.1 million parameters, and 28.7 GFLOPs, YOLOv8 provides

robust performance for mitosis detection tasks. Fine-tuning hyperparameters during training further optimizes its performance.

c) Classification Stage: In this stage, fuzzy-based classification algorithms are applied to distinguish mitotic cells from non-mitotic cells. We selected three classification algorithms for this task. The first, Fuzzy Random Forest (FRF) (Bonissone et al., 2010), is an ensemble method based on fuzzy decision trees. FRF combines the stability of multiple classifier systems with the randomness needed to increase tree diversity, while also utilizing fuzzy logic to handle imperfect data. First, it minimizes bias in random feature selection and addresses some aspects of data imbalance by modifying fuzzy membership degrees based on class distribution. The second algorithm is Fuzzy K-Nearest Neighbors (FKNN), which allocates class membership according to the sample's proximity to members of other classes as opposed to attributing a specific class to data points. This feature enables FKNN to locate memberships of data instances in multiple classes quite effectively in the face of uncertainty and hence improves classification accuracy. Finally, Fuzzy Min-Max (FMM) in a single data pass through the data compound fully performs the learning phase and is applied in either a classification or clustering role. FMM will be working towards fine-tuning and determination of class boundaries by performing three main processes: expansion, overlap testing, and contraction. These fuzzy-based techniques are chosen to manage overlapping classes, uncertainty, and imprecision in the data to ensure an optimal detection system for mitosis in cancer research.

Our motivation to integrate YOLOv8 with fuzzy-based classification methods stems from the need to address the challenges of mitosis detection in histopathological images, such as high inter-class variability, overlapping structures, and staining inconsistencies. YOLOv8, being a state-of-the-art object detection model, offers real-time detection capabilities with high precision and recall. However, due to the ambiguity in distinguishing mitotic figures from similar-looking non-mitotic structures, a conventional threshold-based classification approach may not be sufficient. To mitigate this issue, we incorporated fuzzy classification techniques (Fuzzy Random Forest, Fuzzy K-Nearest Neighbors, and Fuzzy Min-Max) to refine the classification stage. These methods are particularly effective in handling uncertainty and overlapping class boundaries, which are common in mitosis detection. The fuzzy-based classifiers improve robustness by allowing for gradual membership assignment rather than strict binary categorization, enhancing detection performance, as demonstrated by our experimental results.

EXPERIMENT DESIGN

Parameter Settings

Experiments are carried out on a PC with NVIDIA RTX4000 GPU, Intel (R) Xeon (R) W-2245 CPU@3.90GHz, and 64GB System RAM using Python interfaces via Google Colab and Matlab platforms. To assess the effectiveness of the proposed nuclei segmentation methodology, we compare it with the U-Net [54] and DeepLabv3+ (He et al., 2016) architectures. DeepLabv3+ is implemented using five different pretrained models. The motivation for choosing DeepLabv3+ stems from its ability to handle complex segmentation tasks through atrous convolution, which enables capturing multi-scale contextual information and preserving fine details. This makes it particularly well-suited for tasks like nuclei and mitosis detection in biomedical imaging. The parameter settings for the segmentation architectures used in nuclei segmentation are provided in Table 5. Moreover, the parameters for mitosis detection using YOLOv8 include a maximum of 100 epochs, a batch size of 2, a learning rate of 0.0001, and a weight decay of 0.001. The model utilizes a Conv2D stem block with 64 channels, and the optimization is performed using Stochastic Gradient Descent with Momentum (SGDM).

To demonstrate the effectiveness of the proposed nuclei segmentation and mitosis detection methodologies, in addition to the NuSeC and MiDeSeC datasets, two widely used datasets were employed: MoNuSeg 2018 (Kumar et al., 2019) and ICPR 2012. The MoNuSeg 2018 dataset consists of 30 training images representing seven organs (breast, liver, kidney, prostate, bladder, colon, and stomach) with 21,623 manually annotated nuclei, as well as a test set of 14 images from organs like breast, kidney, prostate, bladder, colon, lung, and brain, with 7,223 annotations. Notably, the test set introduces the lung and brain, which are absent in the training data. All images are sourced from patient slides in The Cancer Genome Atlas (TCGA) at a 40× magnification. Annotations were initially created by engineers and verified by an expert pathologist. The ICPR 2012 dataset, designed for mitosis detection in breast cancer histology, includes five H&E-stained images scanned using multiple devices, featuring 50 high power fields (HPFs) and a total of 648 mitotic cell annotations across various scanners. The dataset includes RGB and multispectral images, with ground truth annotations provided by a pathologist.

Table 5. Parameters Settings for Nuclei Segmentation

Parameters	DeepLabv3+	U-Net	CompSegNet
Initial learning rate	0.01	0.01	1,00E-03
Max epochs	100	100	100
Mini batch size	1	1	-
L2 regularization	0.0001	0.0001	-
Momentum	0.9	0.09	-
Gradient threshold	0.05	0.05	-
loss-weight	-	-	α= 0.2
Optimization	SGDM	SGDM	SGDM

Evaluation Metrics

To verify the performance of the nuclei segmentation, we use the following metrics:

a) Dice Coefficient (DC): This metric measures the similarity between the predicted and ground truth segmentation masks and is defined as:

$$Dice = \frac{2\times TP}{(TP+FP)+(TP+FN)} \quad (1)$$

Where TP, FP, and FN represent true positives, false positives, and false negatives, respectively.

b) Aggregated Jaccard Index (AJI): This metric measures the agreement between predicted and ground truth masks, focusing on the shared areas between the masks and penalizing non-overlapping regions. AJI is particularly useful for evaluating algorithms dealing with irregularly shaped objects:

$$AJI = \frac{\sum_{i=1}^{N} G_i \cap S_i}{\sum_{i=1}^{N} G_i \cup S_i + \sum_{S_{k\in U}} S_k} \quad (2)$$

Where N is the number of ground truth nuclei, G_i is the set of ground truth nuclei, S_i is the set of matching segmented nuclei, and S_k is the set of segmented nuclei not matched to any ground truth nuclei. To evaluate the performance of the mitotic detection methodology, we use the following metrics:

c) Precision: This metric measures how accurate the positive predictions are and is defined as:

$$Precision = \frac{TP}{TP+FP} \quad (3)$$

Where TP (True Positive) refers to the count of mitoses that are accurately identified as ground-truth mitoses among those detected, while FP (False Positive) indicates the number of mitoses that are incorrectly identified as ground-truth among the detected mitoses.

c) Recall: This metric represents the fraction of identified mitotic cells out of the total actual mitotic cells:

$$Recall = \frac{TP}{TP+FN} \quad (4)$$

Where FN (False Negative) represents the number of true mitoses that were missed by the detection.

e) F1-score: This metric is the harmonic mean of precision and recall, providing a balanced measure of model performance:

$$F1-Score = 2 \times \frac{Precision \times Recall}{Precision + Recall} \quad (5)$$

EXPERIMENT RESULTS

Results of Nuclei Segmentation

The results for nuclei segmentation across the NuSeC and MoNuSeg datasets are presented in Table 6 in terms of the AJI and DC metrics. The best values are denoted in bold. Furthermore, some visual results of the proposed methodology are provided in Fig. 3.

Table 6. Results on NuSeC and MoNuSeg Datasets

Methods	NuSeC		MoNuSeg	
	AJI	Dice	AJI	Dice
DeepLabv3+ & ResNet50	0.668	0.788	0.680	0.792
DeepLabv3+ & ResNet18	0.654	0.775	0.679	0.785
DeepLabv3+ &Xception	0.648	0.763	0.681	0.768
DeepLabv3+ & MobileNetv2	0.643	0.710	0.650	0.770
DeepLabv3+ & InceptionResNetv2	0.625	0.751	0.654	0.760
U-Net	0.576	0.670	0.645	0.670
Proposed	0.677	0.807	0.705	0.697

The performance of the segmentation methods on the NuSeC dataset varies across different architectures. The proposed methodology demonstrates the strongest results, achieving the highest scores across both the AJI and Dice metrics, indicating its superior ability to segment nuclei in this dataset. Among the DeepLabv3+ variants, the model using ResNet50 closely follows, showing strong performance in capturing the structural details of nuclei. The ResNet18 variant shows good performance, with just a minor drop in accuracy when compared to ResNet50. Other models, like Xception and MobileNetv2, yield relatively lower results, suggesting that these backbones are not as effective for this particular task. Additionally, while the U-Net architecture is often utilized for segmentation, it faces challenges with the NuSeC dataset, resulting in the lowest performance. This indicates that it struggles to manage the complexities of this dataset compared to the more sophisticated DeepLabv3+ and the proposed approach.

The results for the MoNuSeg dataset show a similar trend, with the proposed methodology achieving the highest AJI, which underscores its superior ability to accurately delineate the boundaries of essential factors in nuclei segmentation. Although the Dice coefficient suggests there is some room for improvement in pixel-wise overlap, AJI is the more critical metric for this task, as it more accurately reflects the model's ability to manage boundary detection, a vital component in segmentation challenges like MoNuSeg. Among the DeepLabv3+ models, ResNet50 demonstrates strong performance, with an AJI that is only slightly lower than that of the proposed method, making it a dependable choice for nuclei segmentation. Although ResNet18 outperforms ResNet50 in terms of the Dice coefficient, its slightly lower AJI suggests that it may not capture boundary details as effectively, despite better pixel-level segmentation. Other configurations, such as Xception and MobileNetv2, perform less effectively, with lower AJI values, indicating they struggle more with boundary accuracy. Moreover, the proposed method has lower Dice performance on the MoNuSeg dataset, but AJI is the more critical metric as it better reflects boundary detection, a key challenge in segmentation. AJI assesses segmentation accuracy more reliably by accounting for object-level splitting and merging errors, unlike Dice, which is pixel-based and can be misleading in cases of overlapping or densely packed nuclei. Since MoNuSeg includes nuclei of varying sizes and shapes, Dice may be lower due to minor boundary shifts, while AJI provides a more accurate evaluation. Our analysis shows that the model outperforms existing methods in AJI, with Dice variations mainly influenced by boundary sensitivity.

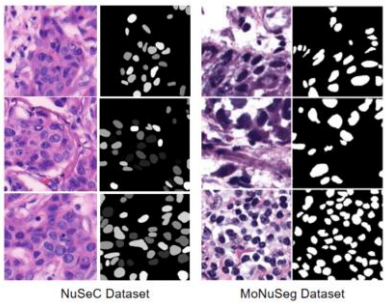

Figure 3. Some visual results of the proposed nuclei segmentation methodology on the NuSeC and MoNuSeg datasets.

Table 7. Comparisons with Recent Studies on MoNuSeg

Reference	AJI	Methods
Li et al., (2019)	0.652	Dual U-Net
Chen et al., (2020)	0.653	REMFA-Net
Guo et al., (2023)	0.703	SAC-Net
Hassan Dinh et al., (2021)	0.7323	Efficient Stain-Aware
Ahmed (2024)	0.652	accurate deep learning
Proposed	0.705	CompSegNet

The results in Table 7 present a comparison of several methods on the MoNuSeg dataset, highlighting their respective AJI scores. The proposed model achieved an AJI score of 0.705, demonstrating its competitive performance in nuclei segmentation. It outperforms methods such as Dual U-Net (0.652) and Efficient Stain-Aware (0.652), which struggle to capture fine-grained details of nuclei in histopathological images, leading to lower segmentation accuracy. REMFA-Net, with an AJI of 0.653, shows a slight improvement over Dual U-Net and Efficient Stain-Aware, but still falls behind the proposed model, possibly due to challenges in multi-scale nuclei segmentation. SAC-Net, achieving an AJI of 0.703, shows an improvement by refining feature maps and enhancing the network's ability to detect smaller nuclei, but does not surpass the proposed model's performance. CompSegNet, with an AJI of 0.705, matches the performance of the proposed model, indicating that both methods are effective for segmentation. However, the proposed model stands out in terms of its ability to handle complex features and segmentation nuances, likely due to specific design choices or techniques aimed at improving performance. Guo et al. (2023) and Hassan Dinh et al. (2021) achieved AJI values of 0.703 and 0.7323, respectively. Hassan Dinh et al.'s method achieved the highest AJI, showing its strength in accurately segmenting nuclei in this challenging dataset. These higher AJI values reflect the ongoing advancements in deep learning models tailored for nuclei segmentation. In conclusion, the proposed model demonstrates competitive performance, matching or exceeding the results of state-of-the-art methods like SAC-Net and CompSegNet. The trend of increasing AJI values highlights the continuous progress in refining deep learning architectures for accurate nuclei segmentation.

Results of Mitosis Detection

The results for mitosis detection across the MiDeSeC and ICPR12 datasets are presented in Table 8 in terms of Precision, Recall, and F1-Score. The best values are denoted in bold. Furthermore, some visual results of the proposed mitosis detection methodology are provided in Figure. 4.

Table 8. Results of Mitosis Detection on MiDeSeC and ICPR12 Datasets

Methods	MiDeSeC			ICPR12		
	Precision	Recall	F1-Score	Precision	Recall	F1-Score
YOLOv8	0.825	0.814	0.819	0.863	0.800	0.831
YOLOv8 + FMM	0.831	0.800	0.815	0.830	0.823	0.826
YOLOv8 + FKNN	0.869	0.860	0.869	0.880	0.870	0.875
YOLOv8 + FRF	0.895	0.870	0.882	0.932	0.894	0.913

For the MiDeSeC dataset, the methodology that combines YOLOv8 with FRF demonstrates the best overall performance, achieving the highest precision and recall, which translates into the best F1-Score of 0.882. This combination significantly outperforms the other methods, with YOLOv8 + FKNN also showing strong performance but trailing behind slightly in all metrics. The standalone YOLOv8 and YOLOv8 + FMM approaches perform similarly, but they fall short compared to the other enhanced methods, indicating that feature refinement techniques like FRF and FKNN are crucial to improve detection accuracy in this dataset. In the ICPR12 dataset, the combination of YOLOv8 and FRF stands out with an impressive F1-Score of 0.913, making it the leading method. This approach's strong precision and recall highlight its effectiveness in accurately identifying mitotic events within the dataset. Although YOLOv8 paired with FKNN also shows commendable performance, achieving an F1-Score of 0.875, it falls short of FRF in both precision and recall. The basic YOLOv8 method demonstrates decent precision but has a slightly lower recall, resulting in an F1-Score of 0.831. On the other hand, YOLOv8 combined with FMM performs a bit worse than the standalone YOLOv8, showing slightly reduced precision and F1-Score, indicating that this

enhancement may not be as effective for the ICPR12 dataset. The F1-Score of 0.913 achieved by the proposed method on the ICPR12 dataset stands out as highly competitive when compared to various studies in the literature. Recent advancements in leading models like YOLO have positioned them at the forefront of object detection. Moreover, running multiple versions of YOLO in parallel and properly scaling the dataset for specific tasks are effective strategies to boost overall performance (Yancey R, 2023). Another method for obtaining cell masks involves using these generated masks to detect mitosis. In the initial processing stage, the Mask R-CNN network creates cell masks. This approach was evaluated using the ICPR12 and ICPR14 datasets. The findings suggest that the masks learned from the smaller ICPR12 dataset can be effectively transferred to the ICPR14 dataset, which does not have cell mask annotations (Sebai et al., 2020). This score reflects the model's balanced precision and recall, showcasing its effectiveness in accurately detecting mitosis events. Achieving an F1-Score above 0.9 in mitosis detection tasks is regarded as a strong outcome, especially on challenging datasets like ICPR12, which feature complex cellular structures. This highlights the robustness and reliability of the proposed methodology in the realm of mitosis detection research.

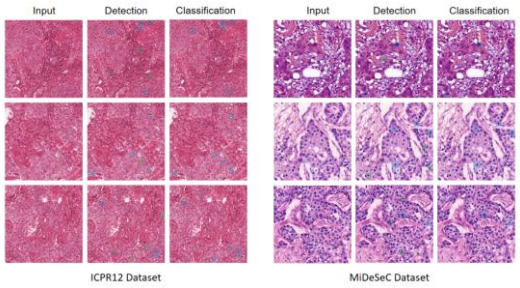

Figure 4. Some visual results of the proposed mitosis detection methodology on ICPR12 dataset. The false positive (FP) and false negative (FN), incorrectly detected, are represented in green, while the true positive (TP), accurately classified, is depicted in blue.

Table 9. Comparisons with Recent Studies on ICPR2012

Reference	F1-Score	Methods
Yancey R, (2023)	0.83	Deep Mitosis
Li et al., (2018)	0.79	ResNet 50 and YOLOv5
Dodballapur et al., (2019)	0.90	Mask R-CNN
Sebai et al., (2020)	0.802	SegMitos
Han et al., (2021)	0.85	PSPNet
Tashk et al., (2020)	0.709	CLBP+SVM
Wang et al., (2021)	0.735	Cascaded ensemble CNN
Proposed	0.913	YOLOv8 + FRF

The proposed method in Table 9, YOLOv8 + FRF, demonstrates superior performance on the ICPR2012 dataset, achieving the highest F1-score of 0.913, which outperforms all other methods. This result highlights the effectiveness of combining the YOLOv8 backbone with the Feature Refinement Framework (FRF), which enhances the model's ability to detect mitotic cells in complex histopathological images. In comparison, other state-of-the-art methods, such as Deep Mitosis (0.83) and ResNet50 + YOLOv5 (0.79), show lower performance, mainly due to their reliance on less refined feature extraction techniques. Mask R-CNN, with an F1-score of 0.90, also performs well but falls short of the proposed method due to challenges in detecting mitotic cells in crowded or textured areas. Similarly, methods like SegMitos (0.802) and PSPNet (0.85) offer reasonable performance but lack the specialized refinement and attention mechanisms that improve the proposed model's accuracy. Traditional methods like CLBP+SVM (0.709) and Cascaded Ensemble CNN (0.735) exhibit lower F1-scores, primarily due to their limitations in capturing fine-grained features of mitotic cells. Overall, the proposed YOLOv8 + FRF method excels in mitosis detection, offering more accurate and robust results in complex histopathological images compared to existing techniques.

CONCLUSION

In this study, we introduced two deep learning methodologies for nuclei segmentation and mitosis detection in histopathological image analysis. Leveraging the CompSegNet architecture for segmentation and combining YOLOv8 with fuzzy-based classification techniques for detection, our approaches achieved high accuracy and robustness across challenging datasets. Another significant contribution of this study is the introduction of two new publicly available datasets, NuSeC and MiDeSeC, designed to support the development and benchmarking of robust models for nuclei segmentation and mitosis detection tasks. These datasets provide a valuable resource for the research community, promoting further advancements in automated histopathological image analysis. Moving forward, our methodologies offer a promising direction for clinical applications, with the potential to enhance diagnostic accuracy in cancer grading and treatment planning. Future work will focus on expanding the datasets and refining the models to improve generalizability and clinical applicability in diverse medical settings.

Acknowledgment

This work is supported by Turkish Scientific and Research Council (TUBITAK) under Grant No.121E379.16.

REFERENCES

Aatresh, A. A., Yatgiri, R. P., Chanchal, A. K., Kumar, A., Ravi, A., Das, D., & Kini, J. (2021). Efficient deep learning architecture with dimension-wise pyramid pooling for nuclei segmentation of histopathology images. *Computerized Medical Imaging and Graphics*, 93, 101975. https://doi.org/10.1016/j.compmedimag.2021.101975.

Amgad, M., Atteya, L. A., Hussein, H., Mohammed, K. H., Hafiz, E., Elsebaie, M. A., & Cooper, L. A. (2022). NuCLS: A scalable crowdsourcing approach and dataset for nucleus classification and segmentation in breast cancer. *GigaScience*, 11, giac037. https://doi.org/10.1093/gigascience/giac037.

Aubreville, M., Stathonikos, N., Bertram, C. A., Klopfleisch, R., Ter Hoeve, N., Ciompi, F., & Breininger, K. (2023). Mitosis domain generalization in histopathology images—the MIDOG challenge. *Medical Image Analysis*, 84, 102699. https://doi.org/10.1016/j.media.2022.102699.

Aubreville, M., Wilm, F., Stathonikos, N., Breininger, K., Donovan, T. A., Jabari, S., & Bertram, C. A. (2023). A comprehensive multi-domain dataset for mitotic figure detection. *Scientific data*, *10*(1), 484. https://doi.org/10.1038/s41597-023-02327-4.

Bankhead, P., Loughrey, M. B., Fernández, J. A., Dombrowski, Y., McArt, D. G., Dunne, P. D., & Hamilton, P. W. (2017). QuPath: Open source software for digital pathology image analysis. *Scientific reports*, 7(1), 1-7. https://doi.org/10.1038/s41598-017-17204-5.

Bertram, C. A., Veta, M., Marzahl, C., Stathonikos, N., Maier, A., Klopfleisch, R., & Aubreville, M. (2020). Are pathologist-defined labels reproducible? Comparison of the TUPAC16 mitotic figure dataset with an alternative set of labels. In *Interpretable and Annotation-Efficient Learning for Medical Image Computing: Third International Workshop, iMIMIC 2020, Second International Workshop, MIL3ID 2020, and 5th International Workshop, LABELS 2020, Held in Conjunction with MICCAI 2020, Lima, Peru, October 4–8, 2020, Proceedings 3*, 204-213. Springer International Publishing. https://doi.org/10.1007/978-3-030-61166-8_22.

Bonissone, P., Cadenas, J. M., Garrido, M. C., & Díaz-Valladares, R. A. (2010). A fuzzy random forest. *International Journal of Approximate Reasoning*, 51(7), 729-747. https://doi.org/10.1016/j.ijar.2010.02.003.

Chen, L. C., Zhu, Y., Papandreou, G., Schroff, F., & Adam, H. (2018). Encoder-decoder with atrous separable convolution for semantic image segmentation. In *Proceedings of the European conference on computer vision (ECCV)*, 801-818. https://doi.org/10.48550/arXiv.1802.02611.

Chen, Y., Li, X., Hu, K., Chen, Z., & Gao, X. (2020). Nuclei segmentation in histopathology images using rotation equivariant and multi-level feature aggregation neural network. In *2020 IEEE International Conference on Bioinformatics and Biomedicine (BIBM)*, 549-554. IEEE. https://doi.org/10.1109/BIBM49941.2020.9313413.

Dodballapur, V., Song, Y., Huang, H., Chen, M., Chrzanowski, W., & Cai, W. (2019). Mask-driven mitosis detection in histopathology images. In *2019 IEEE 16th International Symposium on Biomedical Imaging (ISBI 2019)*, 1855-1859. IEEE. https://doi.org/10.1109/ISBI.2019.8759164.

Gamper, J., Koohbanani, N. A., Benes, K., Graham, S., Jahanifar, M., Khurram, S. A., & Rajpoot, N. (2020). Pannuke dataset extension, insights and baselines. *arXiv preprint arXiv:2003.10778*. https://doi.org/10.48550/arXiv.2003.10778.

Graham, S., Jahanifar, M., Azam, A., Nimir, M., Tsang, Y. W., Dodd, K., & Rajpoot, N. M. (2021). Lizard: A large-scale dataset for colonic nuclear instance segmentation and classification. In *Proceedings of the IEEE/CVF international conference on computer vision*, 684-693. https://doi.org/10.48550/arXiv.2108.11195.

Graham, S., Vu, Q. D., Raza, S. E. A., Azam, A., Tsang, Y. W., Kwak, J. T., & Rajpoot, N. (2019). Hover-net: Simultaneous segmentation and classification of nuclei in multi-tissue histology images. *Medical image analysis*, 58, 101563. https://doi.org/10.1016/j.media.2019.101563.

Hamidinekoo, A., & Zwiggelaar, R. (2017). Stain colour normalisation to improve mitosis detection on breast histology images. In *Deep Learning in Medical Image Analysis and Multimodal Learning for Clinical Decision Support: Third International Workshop, DLMIA 2017, and 7th International Workshop, ML-CDS 2017, Held in Conjunction with MICCAI 2017, Québec City, QC, Canada, September 14, Proceedings 3*, 213-221. Springer International Publishing. https://doi.org/10.1007/978-3-319-67558-9_25.

Hancer, E., Traore, M., Samet, R., Yıldırım, Z., & Nemati, N. (2023). An imbalance-aware nuclei segmentation methodology for H&E stained histopathology images. *Biomedical Signal Processing and Control*, 83, 104720. https://doi.org/10.1016/j.bspc.2023.104720.

Hassan, L., Abdel-Nasser, M., Saleh, A., A. Omer, O., & Puig, D. (2021). Efficient stain-aware nuclei segmentation deep learning framework for multi-center histopathological images. *Electronics*, 10(8), 954. https://doi.org/10.3390/electronics10080954.

He, K., Zhang, X., Ren, S., & Sun, J. (2016). Deep residual learning for image recognition. In *Proceedings of the IEEE conference on computer vision and pattern recognition*, 770-778. https://doi.org/10.1109/CVPR.2016.90.

Hlavcheva, D., Yaloveha, V., & Podorozhniak, A. (2019). Application of convolutional neural network for histopathological analysis. *Advanced Information Systems*, *3*(4), 69-73. https://doi.org/10.20998/2522-9052.2019.4.10.

Hoorali, F., Khosravi, H., & Moradi, B. (2022). Automatic microscopic diagnosis of diseases using an improved UNet++ architecture. *Tissue and Cell*, *76*, 101816. https://doi.org/10.1016/j.tice.2022.101816.

Ilyas, T., Mannan, Z. I., Khan, A., Azam, S., Kim, H., & De Boer, F. (2022). TSFD-Net: Tissue specific feature distillation network for nuclei segmentation and classification. *Neural Networks*, 151, 1-15. https://doi.org/10.1016/j.neunet.2022.02.020.

Jahanifar, M., Shephard, A., Zamanitajeddin, N., Raza, S. E. A., & Rajpoot, N. (2022). Stain-robust mitotic figure detection for MIDOG 2022 challenge. *arXiv preprint arXiv:2208.12587*. https://doi.org/10.1016/j.media.2024.103132.

Jiang, S., & Li, J. (2022). TransCUNet: UNet cross fused transformer for medical image segmentation. *Computers in Biology and Medicine*, 150, 106-207. https://doi.org/10.1016/j.compbiomed.2022.106207.

Khan, M. S., Ali, S., Lee, Y. R., Kang, M. K., Park, S. Y., Tak, W. Y., & Jung, S. K. (2023). TransUNet-lite: A robust approach to cell nuclei segmentation. In *Proceedings of the 2023 7th International Conference on Medical and Health Informatics*, 251-258. https://doi.org/10.1145/3608298.3608344.

Khan, H. U., Raza, B., Shah, M. H., Usama, S. M., Tiwari, P., & Band, S. S. (2023). SMDetector: Small mitotic detector in histopathology images using faster R-CNN with dilated convolutions in backbone model. *Biomedical Signal Processing and Control*, 81, 104-414. https://doi.org/10.1016/j.bspc.2022.104414.

Khan, M. Z., Gajendran, M. K., Lee, Y., & Khan, M. A. (2021). Deep neural architectures for medical image semantic segmentation. *IEEE Access*, 9, 83002-83024. https://doi.org/10.1109/ACCESS.2021.3086530.

Kumar, N., Verma, R., Anand, D., Zhou, Y., Onder, O. F., Tsougenis, E., & Sethi, A. (2019). A multi-organ nucleus segmentation challenge. *IEEE transactions on medical imaging*, 39(5), 1380-1391. https://doi.org/10.1109/TMI.2019.2947628.

Kumar, N., Verma, R., Sharma, S., Bhargava, S., Vahadane, A., & Sethi, A. (2017). A dataset and a technique for generalized nuclear segmentation for computational pathology. *IEEE transactions on medical imaging*, 36(7), 1550-1560. https://doi.org/10.1109/TMI.2017.2677499.

Le Dinh, T., Lee, S. H., Kwon, S. G., & Kwon, K. R. (2022). Cell nuclei segmentation in cryonuseg dataset using nested unet with efficientnet encoder. In *2022 International Conference on Electronics, Information, and Communication (ICEIC)*, 1-4. IEEE. https://doi.org/10.1109/ICEIC54506.2022.9748537.

Li, C., Wang, X., Liu, W., & Latecki, L. J. (2018). DeepMitosis: Mitosis detection via deep detection, verification and segmentation networks. *Medical image analysis*, 45, 121-133. https://doi.org/10.1016/j.media.2017.12.002.

Liu, X., Guo, Z., Cao, J., & Tang, J. (2021). MDC-net: A new convolutional neural network for nucleus segmentation in histopathology images with distance maps and contour information. *Computers in Biology and Medicine*, 135, 104543. https://doi.org/10.1016/j.compbiomed.2021.104543.

Ludovic, R., Daniel, R., Nicolas, L., Maria, K., Humayun, I., Jacques, K., & Catherine, G. (2013). Mitosis detection in breast cancer histological images An ICPR 2012 contest. *Journal of pathology informatics*, 4(1), 8. https://doi.org/10.4103/2153-3539.112693.

Maarouf, C., Benomar, M. L., & Settouti, N. (2021). Pre-trained backbones effect on nuclei segmentation performance. In *Mediterranean Conference on Pattern Recognition and Artificial Intelligence*, 108-118. Cham: Springer International Publishing. https://doi.org/10.1007/978-3-031-04112-9_8.

Macenko, M., Niethammer, M., Marron, J. S., Borland, D., Woosley, J. T., Guan, X., & Thomas, N. E. (2009). A method for normalizing histology slides for quantitative analysis. In *2009 IEEE international symposium on biomedical imaging: from nano to macro*, 1107-1110. IEEE. https://doi.org/10.1109/ISBI.2009.5193250.

Mahbod, A., Schaefer, G., Bancher, B., Löw, C., Dorffner, G., Ecker, R., & Ellinger, I. (2021). CryoNuSeg: A dataset for nuclei instance segmentation of cryosectioned H&E-stained histological images. *Computers in biology and medicine*, *132*, 104-349. https://doi.org/10.1016/j.compbiomed.2021.104349.

Maroof, N., Khan, A., Qureshi, S. A., ul Rehman, A., Khalil, R. K., & Shim, S. O. (2020). Mitosis detection in breast cancer histopathology images using hybrid feature space. *Photodiagnosis and photodynamic therapy*, *31*, 101-885. https://doi.org/10.1016/j.pdpdt.2020.101885.

Naylor, P., Laé, M., Reyal, F., & Walter, T. (2017). Nuclei segmentation in histopathology images using deep neural networks. In *2017 IEEE 14th international symposium on biomedical imaging (ISBI 2017)*, 933-936. IEEE. https://doi.org/10.1109/ISBI.2017.7950669.

Naylor, P., Laé, M., Reyal, F., & Walter, T. (2018). Segmentation of nuclei in histopathology images by deep regression of the distance map. *IEEE transactions on medical imaging*, 38(2), 448-459. https://doi.org/10.1109/TMI.2018.2865709.

Nemati, N., Samet, R., Hancer, E., Yildirim, Z., & Akkas, E. E. (2023). A Hybridized Deep Learning Methodology for Mitosis Detection and Classification from Histopathology Images. *Journal of Machine Intelligence and Data Science (JMIDS)*, *4*(1), 35-43. https://doi.org/10.11159/jmids.2023.005.

Obeid, A., Mahbub, T., Javed, S., Dias, J., & Werghi, N. (2022). NucDETR: end-to-end transformer for nucleus detection in histopathology images. In *International Workshop on Computational Mathematics Modeling in Cancer Analysis*, 47-57. Cham: Springer Nature Switzerland. https://doi.org/10.1007/978-3-031-17266-3_5.

Qin, J., He, Y., Zhou, Y., Zhao, J., & Ding, B. (2022). REU-Net: Region-enhanced nuclei segmentation network. *Computers in Biology and Medicine*, 146, 105-546. https://doi.org/10.1016/j.compbiomed.2022.105546.

Ronneberger, O., Fischer, P., & Brox, T. (2015). U-net: Convolutional networks for biomedical image segmentation. In *Medical image computing and computer-assisted intervention–MICCAI 2015: 18th international conference, Munich, Germany, October 5-9, 2015, proceedings*, 3(18), 234-241. Springer International Publishing. https://doi.org/10.48550/arXiv.1505.04597.

Roux, L., Racoceanu, D., Capron, F., Calvo, J., Attieh, E., Le Naour, G., & Gloaguen, A. (2014). Mitos & atypia. *Image Pervasive Access Lab (IPAL), Agency Sci., Technol. & Res. Inst. Infocom Res., Singapore, Tech. Rep*, 1, 1-8.

Sebai, M. (2020). Improved SegMitos framework for mitosis detection in breast cancer histopathology images. In *2020 IEEE International Conference on Artificial Intelligence and Information Systems (ICAIIS)*, 102-106. IEEE. https://doi.org/10.1109/ICAIIS49377.2020.9194877.

Sebai, M., Wang, T., & Al-Fadhli, S. A. (2020). PartMitosis: a partially supervised deep learning framework for mitosis detection in breast cancer histopathology images. *IEEE Access*, 8, 45133-45147. https://doi.org/10.1109/ACCESS.2020.2978754.

Sirinukunwattana, K., Raza, S. E. A., Tsang, Y. W., Snead, D. R., Cree, I. A., & Rajpoot, N. M. (2016). Locality sensitive deep learning for detection and classification of nuclei in routine colon cancer histology images. *IEEE transactions on medical imaging*, *35*(5), 1196-1206. https://doi.org/10.1109/TMI.2016.2525803.

Sohail, A., Khan, A., Wahab, N., Zameer, A., & Khan, S. (2021). A multi-phase deep CNN based mitosis detection framework for breast cancer histopathological images. *Scientific Reports*, 11(1), 6215. https://doi.org/10.1038/s41598-021-85652-1.

Swarts, D. R., van Suylen, R. J., den Bakker, M. A., van Oosterhout, M. F., Thunnissen, F. B., Volante, M., & Speel, E. J. M. (2014). Interobserver variability for the WHO classification of pulmonary carcinoids. *The American journal of surgical pathology*, *38*(10), 1429-1436. https://doi.org/10.1097/PAS.0000000000000300.

Traoré, M., Hancer, E., Samet, R., Yıldırım, Z., & Nemati, N. (2024). CompSegNet: An enhanced U-shaped architecture for nuclei segmentation in H&E histopathology images. *Biomedical Signal Processing and Control*, *97*, 106699. https://doi.org/10.1016/j.bspc.2024.106699.

Verdicchio, M., Brancato, V., Cavaliere, C., Isgrò, F., Salvatore, M., & Aiello, M. (2023). A pathomic approach for tumor-infiltrating lymphocytes classification on breast cancer digital pathology images. *Heliyon*, *9*(3). https://doi.org/10.1016/j.heliyon.2023.e14371.

Verma, R., Kumar, N., Patil, A., Kurian, N. C., Rane, S., Graham, S., & Sethi, A. (2021). MoNuSAC2020: A multi-organ nuclei segmentation and classification challenge. *IEEE Transactions on Medical Imaging*, 40(12), 3413-3423. https://doi.org/10.1109/TMI.2021.3085712.

Veta M, Viergever MA, Pluim JPW, Stathonikos N, van Diest PJ. MICCAI Grand Challenge: Assessment of mitosis detection algorithms (AMIDA13). Computer Vision and Pattern Recognition 2014. https://doi.org/10.1016/j.media.2014.11.010.

Vu, Q. D., Graham, S., Kurc, T., To, M. N. N., Shaban, M., Qaiser, T., & Farahani, K. (2019). Methods for segmentation and classification of digital microscopy tissue images. *Frontiers in bioengineering and biotechnology*, 7, 53. https://doi.org/10.3389/fbioe.2019.00053.

Wilm, F., Marzahl, C., Breininger, K., & Aubreville, M. (2021). Domain adversarial RetinaNet as a reference algorithm for the MItosis DOmain generalization challenge. In *International Conference on Medical Image Computing and Computer-Assisted Intervention*, 5-13. Cham: Springer International Publishing. https://doi.org/10.48550/arXiv.2108.11269.

Wolberg, W. (1992). Breast cancer Wisconsin (original). *UCI Machine Learning Repository*, 110. https://doi.org/10.24432/C5HP4Z.

Yancey, R. (2023). Parallel YOLO-based Model for Real-time Mitosis Counting. 10.24132/CSRN.3201.32.

Yancey, R. E. (2022). Deep Feature Fusion for Mitosis Counting. In *2022 3rd International Conference on Pattern Recognition and Machine Learning (PRML)*, 151-158. IEEE. https://doi.org/10.1109/PRML56267.2022.9882245.

Yang, G., Huang, J., He, Y., Chen, Y., Wang, T., Jin, C., & Sengphachanh, P. (2022). GCP-Net: A Gating Context-Aware Pooling Network for Cervical Cell Nuclei Segmentation. *Mobile Information Systems*, 2022(1), 7511905. https://doi.org/10.1155/2022/7511905.